Letters

DC Output Ripple Suppression of High-Frequency DC–DC Resonant Converter

Xingkui Mao, *Member, IEEE*, Junhui Zhou, *Graduate Student Member, IEEE*, Binyi Zhang, *Student Member, IEEE*, Youtu Lin, Jiqing Dong, *Member, IEEE*, Yueshi Guan, *Senior Member, IEEE*, and Yiming Zhang, *Senior Member, IEEE*

***Abstract*—Increasing switching frequency can greatly improve power density of dc–dc power converter, while meets challenges of significant high-frequency dc output ripple. The capacitor filter is a most cost-effective suppression for the output ripple. However, the capacitor parasitic parameters will deteriorate the suppression. The frequency characteristic of the capacitor filter was analyzed by considering the parasitic parameters. Then, a novel parallel dual capacitors filer is proposed, which creates the reverse coupling between the two adjacent capacitors of the filter by constructing opposite current flowing through the capacitors. Using the novel dual capacitors filer as a cell, a novel compact multicapacitors filer of V-shape is further extended. The insert gain test and the prototype with 20 MHz of switching frequency are constructed, and the experiments verified that the novel filters suppress the ripple by maximum about 50% comparing with the traditional capacitor without adding volume and cost.**

***Index Terms*—Capacitor filter, dc high-frequency ripple, dc–dc resonant converter.**

I. Introduction

INCREASING switching frequency of dc–dc power converters is beneficial for reducing volume and weight of passive components, greatly improving power density of the converter [1]. However, many challenges will arise with switching frequency increasing up to several and tens of MHz, such as higher switching loss, parasitic parameters effect, and manufacturing consistence. Topics of main circuit resonant topology and design [2], [3], driving [4], control [5], and magnetic material and components [6] had been researched quite extensively. Moreover, the output of the converters exhibits significant high-frequency dc ripple. The dc capacitor filter is most cost-effective suppressing for the ripple. However, it is found that even though the dc filters are paralleled with much more pieces of capacitors of low equivalent series inductance (ESL), such as MLCC capacitor, the dc ripple cannot be further suppressed effectively. The frequency characteristic should be researched for the dc filter under several and tens of MHz.

Under low switching frequency of several hundreds of kHz (comparing to tens of MHz), the dc–dc converter output ripple can be easily reduced by the traditional filter with more parallel capacitors, and the relative research of the ripple suppressing is not quite necessary. However, the dc output ripple is difficult to be reduced under high switching frequency with up to several and tens of MHz. Except for unsatisfying for the ripple coefficient requirement, it can also be seen that the large dc output ripple will make the high-frequency dc–dc resonant converter to be susceptible to instability under common-used ON–OFF or hysteresis control [5].

Comparing to the dc ripple of the output end, the conducted EMI noise is in the input end, and there is similar issue under the high frequency of tens of MHz. In the conducted noise EMI filter, parasitic (including self- and mutual parasitic) parameters will deteriorate noise attenuation at high-frequency range [7]. Designing of the parasitic parameters is a key topic of improving the conducted EMI filter performance. There are many litterateurs on this effect research, especially on parasitic mutual inductance caused by near magnetic field coupling [7], [8], [9], [10], [11], [12]. Wang et al. [7] proposed a classic method of introducing negative mutual inductance to cancel ESL of the conducted EMI filter capacitors. Methods of conducted EMI filter components arrangement [9], and combination with printed circuit board (PCB) layout [10], shielding of metallic and ferrite sheets [11], and cross-parallel connection [12] are proposed to minimize adverse impact of the parasitic parameters. Comparing with the conducted noise filter, the output dc filter needs more parallel capacitors and endures higher frequency ripple.

This brief models and analyzes frequency characteristic of the dc capacitor filter by considering parasitic parameters first, then proposes a novel compact parallel capacitors filter by constructing reverse mutual coupling of the adjacent capacitors to improve the filter dc suppressing.

Manuscript received 24 August 2023; revised 12 October 2023; accepted 30 October 2023. Date of publication 6 November 2023; date of current version 22 December 2023. This work was supported in part by the National Natural Science Foundation of China under Grant 51207025. *(Corresponding author: Xingkui Mao.)*

Xingkui Mao, Junhui Zhou, Binyi Zhang, Youtu Lin, Jiqing Dong, and Yiming Zhang are with the College of Electrical Engineering and Automation, Fuzhou University, Fuzhou 350108, China (e-mail: mxk782@fzu.edu.cn; 220120043@fzu.edu.cn; 210120075@fzu.edu.cn; 210127176@fzu.edu.cn; dongjiqing@fzu.edu.cn; zym@fzu.edu.cn).

Yueshi Guan is with the Harbin Institute of Technology, Harbin 150001, China (e-mail: guanyueshi@hit.edu.cn).

Color versions of one or more figures in this article are available at https://doi.org/10.1109/TPEL.2023.3329796.

Digital Object Identifier 10.1109/TPEL.2023.3329796

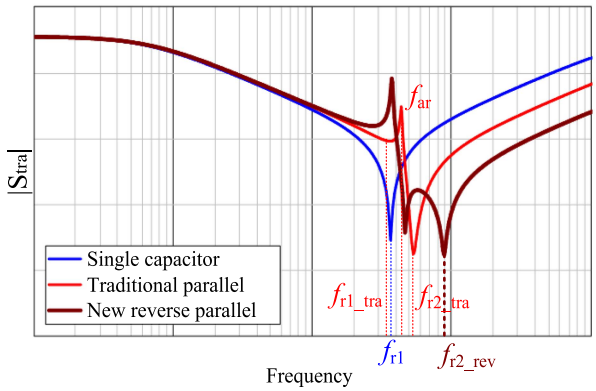

Fig. 1. Insert gain magnitude of a single capacitor, the traditional simple dual capacitors filter, and the new reverse parallel dual capacitors filter.

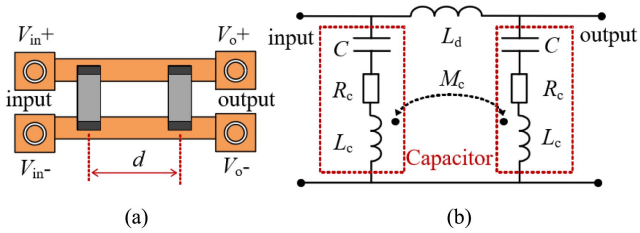

Fig. 2. Traditional simple parallel dual capacitors filter. (a) Layout diagram. (b) Equivalent circuit.

II. Frequency Characteristics of Capacitor Filter

The typical insert gain of a single capacitor or single capacitor filter is shown Fig. 1 with blue line. Due to the ESL of self-parasitic parameters, the capacitor exhibits inductive characteristic to deteriorate filtering above resonant frequency of f_{r1}. As to the dual or multiple capacitors filter, the parasitic mutual coupling must be considered in addition to ESL. The equivalent circuit of the traditional simple parallel dual capacitors filter was constructed by considering M_{c} and L_{d} as Fig. 2, where R_{c} and L_{c} are equivalent series resistance and ESL of a single capacitor C, and L_d is the PCB trace inductance between the adjacent capacitors with distance d, and M_{c} is the mutual-parasitic inductance between the adjacent capacitors. V_{in} and V_{o} are the input and output of the capacitor filter. Because the capacitors are placed to be perpendicular to the PCB trace, the mutual coupling between the capacitors and the trace is neglected. The insert gain S_{tra} of the traditional dual capacitors filter can be deduced from the principle of [13]:

$$S_{\mathrm{tra}} = 2RK_1/K_2K_3 \tag{1}$$

where R is the 50 Ω of network analyzer internal impedance in insert gain measurement, and ω is the angular frequency, and

$$K_1 = \omega^4C^2(L_{\mathrm{c}}^2 - M_{\mathrm{c}}^2 + L_{\mathrm{d}}M_{\mathrm{c}}) - 2\omega^2L_{\mathrm{c}}C + 1$$
$$K_2 = \omega RC + \mathrm{j}[\omega^2C(L_{\mathrm{c}} + M_{\mathrm{c}}) - 1]$$
$$K_3 = [\omega^3L_{\mathrm{d}}C(L_{\mathrm{c}} - M_{\mathrm{c}}) - \omega L_{\mathrm{d}}] - 2\mathrm{j}R[\omega^2C(L_{\mathrm{c}} + L_{\mathrm{d}}/2 - M_{\mathrm{c}}) - 1].$$

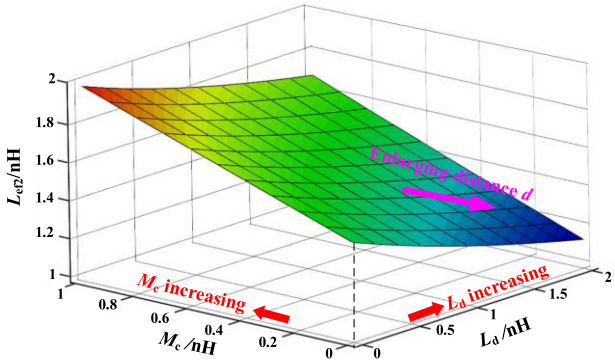

Fig. 3. L_{ef2} vs. M_{c} and L_{d} of the traditional DC capacitor filter.

The insert gain magnitude curve can be depicted based on (1), as shown in Fig. 1. It can be observed that there are two resonance points of $f_{\mathrm{r1\_tra}}$ and $f_{\mathrm{r2\_tra}}$, and one antiresonance point of f_{ar}. In frequency range of $f > f_{\mathrm{r2\_tra}}$, the capacitor filter exhibits inductive characteristics, which can be represented by the effective inductance L_{ef2} of (2) deduced by the asymptote of the insert gain curve $|S_{\mathrm{tra}}|$ during the above frequency $f_{\mathrm{r2\_tra}}$. We can see that the higher $f_{\mathrm{r2\_tra}}$ and the smaller L_{ef2}, the stronger of the insert gain or better attenuation of the ripple in high-frequency range is obtained for the capacitor filter

$$L_{\mathrm{ef2}} = \frac{L_{\mathrm{c}} + M_{\mathrm{c}}\left(\frac{L_{\mathrm{d}}}{L_{\mathrm{c}} - M_{\mathrm{c}}} + 1\right)}{2\left(\frac{L_{\mathrm{d}}}{2(L_{\mathrm{c}} - M_{\mathrm{c}})} + 1\right)}. \tag{2}$$

Based on (2), the relationship among L_{ef2}, M_{c}, and L_{d} can be depicted as Fig. 3. It can be seen that L_{ef2} increases with increasing of M_{c}, while decreases with increasing of L_{d}, but the impact of M_{c} is more apparent. In fact, the M_{c} and L_{d} are reversely dependent variables (larger L_{d} and smaller M_{c} showing by pink arrow) on d. So the larger adjacent distance d, which makes smaller M_{c} of loose coupling and larger L_{d}, will result in a smaller effective inductance and improve filtering or suppressing ripple performance. Even though the larger distance d can be benefit of better suppressing ripple, it will result in a larger filter layout size, and is not preferred.

III. Novel Capacitor Filter

A. Reverse Parallel Dual Capacitors

A novel reverse compact parallel dual capacitors filter is proposed, whose layout and equivalent circuit are shown in Fig. 4. This compact structure ensures that the high-frequency current flowing through the two capacitors has opposite direction, creating a reverse-coupling effect between them. In addition, the reverse structure makes PCB trace increasing, which introduces a larger L_d, improving the coupling inductance M_t between the PCB trace and the capacitors.

The capacitor filter insert gain S_{rev} can be deduced through an equivalent transformation of the circuit in Fig. 4(b)

$$S_{\mathrm{rev}} = 2RM_1/M_2M_3 \tag{3}$$

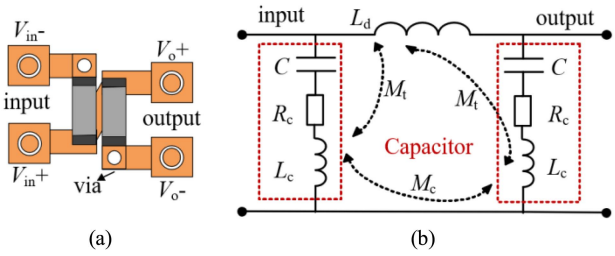

Fig. 4. Novel reverse parallel dual capacitors filter. (a) Layout diagram. (b) Equivalent circuit.

where

$$M_1 = \omega^4 C^2 (L_c^2 - M_c^2 + M_t^2 - 2L_c M_t + 2M_c M_t + L_d M_c) - 2\omega^2 C(L_c - M_t) + 1$$

$$M_2 = \omega^2 C(L_c - M_t) - 1 - j\omega RC$$

$$M_3 = 2R\left[\omega^2 C\left(L_c + \frac{L_d}{2} + M_c - 2M_t\right) - 1\right] - j\left[\omega^3 C(M_t^2 - L_d M_c - L_c L_d) + \omega L_d\right].$$

The insert gain magnitude curve of the new reverse parallel capacitors filter can also be depicted as Fig. 1 based on (3). And the resonance frequency f_{r2_rev} can be obtained by setting S_{rev} tend to be infinitesimal

$$f_{r2\_rev} = \frac{1}{2\pi\sqrt{\left[L_c' - M_c - \sqrt{M_c(M_c + L_d')}\right] C}}. \quad (4)$$

The effective inductance L_{ef3} above f_{r2_rev} can be obtained like (2) by the asymptote of the insert gain $|S_{rev}|$ curve

$$L_{ef3} = \frac{L_c' - M_c\left(\frac{L_d'}{L_c'} + 2\right)}{2\left(\frac{L_d'}{2L_c'} + 1\right)} \quad (5)$$

where $L_c' = L_c - M_t + M_c$ and $L_d' = L_d - 2M_t$. The curve shows that the reverse coupling M_c makes smaller L_{ef2} and higher f_{r2_rev}, resulting in better suppressing performance of the new capacitor filter. This improvement is realized by utilizing the reverse coupling of parasitic parameters, and without adding volume and cost of the capacitor filters with compact structure.

The relationship among L_{ef3}, M_c, M_t, and L_d can be depicted as Fig. 5. It can be seen that L_{ef3} decreases with increasing of M_c and M_t, and L_{ef3} also decreases with the increasing of L_d and M_t except the zone with pink dot line. In fact, because the L_d and M_t are positive dependent variables on d, that is, larger d makes larger L_d and larger M_t at same time, the L_d and M_t will not happen in the pink line zone. Moreover, smaller d will make larger M_c, so the new filter can improve the suppression without enlarging the distance d, while by reverse coupling.

B. Reverse Parallel Multicapacitors

As to multicapacitors filter, the mutual coupling or the parasitic parameters will be more complex. Based on the above

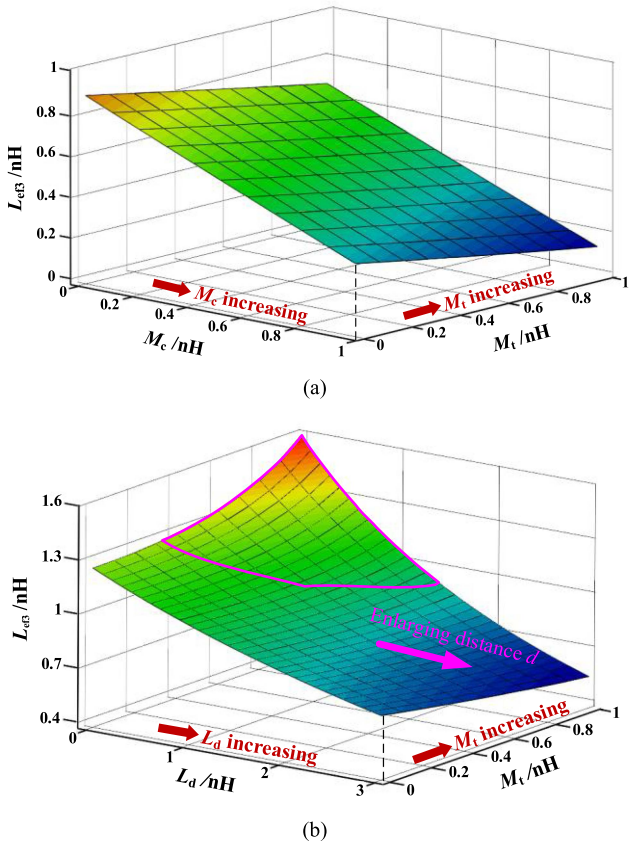

Fig. 5. L_{ef3} of the novel capacitor filter vs. (a) M_c and M_t. (b) L_d and M_t.

reverse parallel concept, a novel reverse compact parallel multicapacitors filter is proposed by using the above reverse parallel dual capacitors filter as an extended cell. In the new structure, the adjacent dual capacitors marked with blue dot line is parallel connected reversely, so the any three adjacent capacitors form either a V-shaped or an inverted V-shaped structure, as shown in Fig. 6(a). This structure layout introduces reverse coupling between each pair of adjacent capacitors along horizontal axis.

In order to improve current handling capacity of the filter, an additional group of reverse parallel capacitors is further proposed, which is in a vertical mirror arrangement for multicapacitors parallel filter, as shown in Fig. 6(b). Because this structure adopts two groups of parallel PCB trace, it can shorten the filters PCB trace, and make the output current flow through the two parallel PCB trace, resulting in lower trace loss, and handling higher current. The same analysis can be carried out for the proposed multicapacitors filter because it is an extension of the proposed reverse parallel dual capacitors filter. The novel filter is very compact.

IV. Experimental Verification

A. Insert Gain Test

The insert gain magnitude test by the network analyzer Agilent E5072A is shown as Fig. 7. It can be seen that there exists two resonance points and one antiresonance point. Based on the

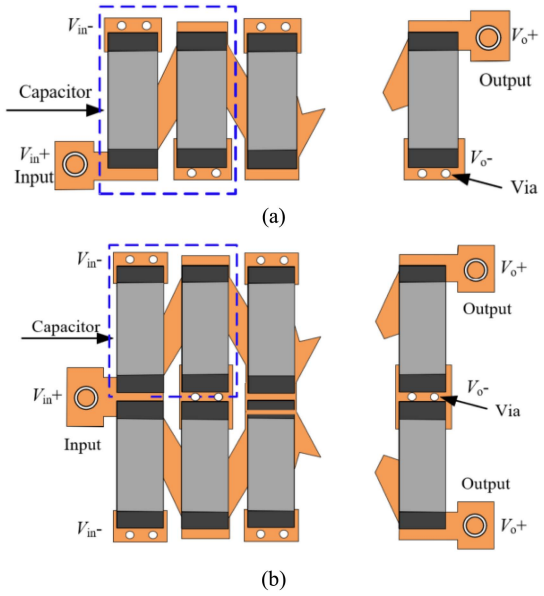

Fig. 6. Novel revers parallel multicapacitors filter. (a) V-shaped structure. (b) Vertical mirror V-shaped structure.

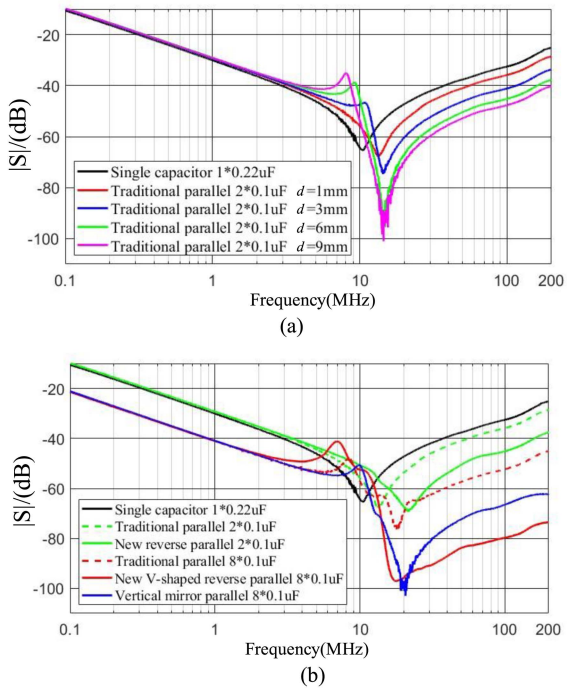

Fig. 7. Insert gain test. (a) Versus distance d. (b) Versus different structures.

insert gain test, the effective inductance $L_{\rm ef}$ can be further calculated as in Fig. 8. The test verifies the above analysis and shows that small coupling of the larger distance d in the traditional filter of Fig. 7(a), and the novel reverse coupling between the adjacent capacitors will improve the resonant frequency $f_{\rm r2\_rev}$ and reducing the effective inductance $L_{\rm ef3}$ in Figs. 7(b) and 8, then improving the suppressing performance of the capacitor filter in high-frequency range. The test is with MLCC capacitor

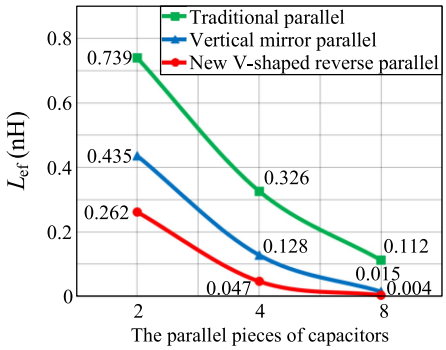

Fig. 8. $L_{\rm ef}$ versus parallel pieces of capacitors of the different capacitor filter.

TABLE I
PARAMETERS OF EXPERIMENTAL PROTOTYPE

$Q_{\rm main}$	GS61008T	$Q_{\rm SR}$	EPC2015C	$L_{\rm F}$	33 nH
$C_{\rm F}$	810 pF	$C_{\rm B}$	0.6 μF	$C_{\rm rec}$	667 pF
$L_{\rm R}$	27 nH	$C_{\rm R}$	540 pF	$C_{\rm O}$	2*10 μF
$C_{\rm Fil}$	0.1 μF*12	L_{11}	40.3 nH	L_2	85 nH
k	0.816	-	-	-	-

of AVX corporation. In the mark box of Fig. 7, 2*0.1 μF means two pieces of parallel capacitors with 0.1 μF capacitance.

B. DC/DC Converter Verification

The high-frequency dc/dc resonant converter prototype adopts topology of isolated Class Φ2 inverter and Class E rectifier of Fig. 9, and ON–OFF control. The prototype is with input 18 V, output 5 V/2 A, switching frequency of 20 MHz, and ON–OFF frequency of 40 kHz. $C_{\rm O}$ is the energy storage capacitor, and $C_{\rm Fil}$ is the dc capacitors filter. L_{11}, L_{22}, and k are equivalent T-model parameters of the air-core transformer T. Detailed parameters are given in Table I.

In the experiments, the three capacitor filters of Fig. 9(c) were separately embedded in section of output capacitor filter in main board by the pins. Fig. 9(c) gives the three capacitor filters of the traditional parallel structure of Fig. 2, the V-shaped parallel structure of Fig. 6(a), and the vertical mirror parallel structure of Fig. 6(b) in the experiments. Each filter is paralleled with 12 pieces of MLCC capacitor 0.1 μF of AVX corporation, and the respective PCB layouts are also given. In the traditional parallel structure, the single layer PCB is used, and the double layer PCB is designed for the other two structures. The top layer and bottom layer is for $V_{\rm o+}$ and $V_{\rm o-}$, respectively, and the twisting trace of $V_{\rm o+}$ and $V_{\rm o-}$ is realized by the via. In order to make fair comparisons, the PCB trace width and the traditional parallel structure distance d between the adjacent capacitors are also designed to be same in the three capacitors.

The output voltage ripple is measured as given in Fig. 10 under full-load and close-loop ON–OFF control. The output ripple is 610, 300, and 390 mV for the above different capacitor filters, respectively. The novel capacitor filters effectively suppress the

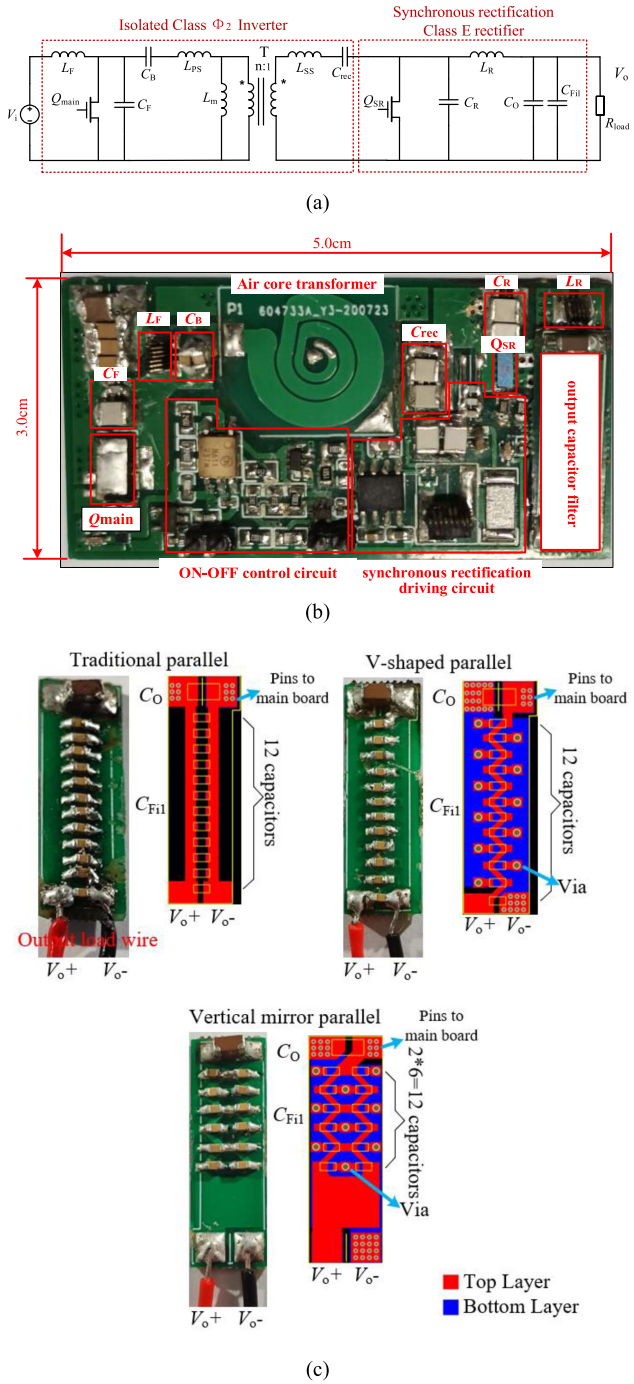

Fig. 9. Prototype. (a) Main circuit topology. (b) DC–DC converter. (c) Three capacitor filters and its PCB layout (12 pieces parallel of 0.1 μF).

ripple by maximum about 50% comparing with the traditional capacitor.

Because the PCB trace length of the different filter structures is not same, the trace loss will be different. But it is just slightly different because the dc filter is paralleled with energy storage bulky MLCC capacitor C_o of 20 μF, and most of the high-frequency ac component of the output current follows through

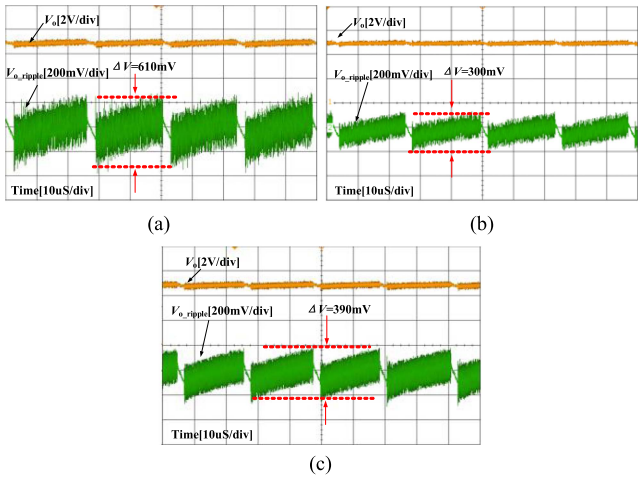

Fig. 10. Experimental waveforms of output voltage @ full-load for the three filters. (a) Traditional parallel filters. (b) New V-shaped reverse parallel filters. (c) Vertical mirror reverse parallel filters.

the C_o, resulting in only suppressing the small output ripple for the filter. The measured efficiency at full load (5 V/2 A) is 78.51%, 78.4%, and 78.7% for the traditional parallel, V-shaped parallel, and vertical mirror parallel structure, respectively, and this also proves that the filter of vertical mirror structure can improve current handling capacity.

IV. Conclusion

The self- and mutual-parasitic parameters will deteriorate suppressing performance of the dc output capacitor filter under up to tens of MHz frequency. The model and analysis reveal that the small mutual coupling of the larger adjacent distance will improve filtering performance of the higher resonance frequency and the smaller effective inductance in the traditional filter. The proposed novel dual capacitors dc filter introduces reverse coupling by constructing current flowing through the adjacent capacitors with opposite directions, improving the resonance frequency and reducing the effective inductance. Using the novel dual capacitors filer as a cell, a novel multicapacitors filer of V-shaped structure and vertical mirror V-shaped structure are further extended. The experiments verify the analysis and the effective suppressing ripple by maximum about 50% of the novel capacitor filter. The novel dc filter is very compact and without adding volume and cost.

References

[1] Z. Tong, L. Gu, and J. Rivas-Davila, "Wideband PPT class Φ2 inverter using phase-switched impedance modulation and reactance compensation," *IEEE Trans. Ind. Electron.*, vol. 69, no. 6, pp. 5724–5734, Jun. 2022.

[2] C. Liu, Y. Guan, Y. Wang, J. M. Alonso, and D. Xu, "Coordinate compression strategy of resistance and reactance for MHz-range inverter system," *IEEE Trans. Power Electron.*, vol. 37, no. 12, pp. 14993–15004, Dec. 2022.

[3] Y. Guan, C. Liu, Y. Wang, W. Wang, and D. Xu, "Analytical derivation and design of 20-MHz DC–DC soft-switching resonant converter," *IEEE Trans. Ind. Electron.*, vol. 68, no. 1, pp. 210–221, Jan. 2021.

[4] L. Gu, Z. Tong, W. Liang, and J. Rivas-Davila, "A multi-resonant gate driver for high-frequency resonant converters," *IEEE Trans. Ind. Electron.*, vol. 67, no. 2, pp. 1405–1414, Feb. 2020.

[5] Y. Li and X. Ruan, "Output current limitation for ON–OFF controlled very-high-frequency class E DC–DC converter," *IEEE Trans. Ind. Electron.*, vol. 69, no. 11, pp. 11826–11831, Nov. 2022.

[6] R. S. Yang, A. J. Hanson, B. A. Reese, C. R. Sullivan, and D. J. Perreault, "A low-loss inductor structure and design guidelines for high-frequency applications," *IEEE Trans. Power Electron.*, vol. 34, no. 10, pp. 9993–10005, Oct. 2019.

[7] S. Wang, F. C. Lee, and W. G. Odendaal, "Cancellation of capacitor parasitic parameters for noise reduction application," *IEEE Trans. Power Electron.*, vol. 21, no. 4, pp. 1125–1132, Jul. 2006.

[8] P. González-Vizuete, F. Fico, A. Fernández-Prieto, M. J. Freire, and J. B. Mendez, "Calculation of parasitic self- and mutual-inductances of thin-film capacitors for power line filters," *IEEE Trans. Power Electron.*, vol. 34, no. 1, pp. 236–246, Jan. 2019.

[9] B. J. Pierquet, T. C. Neugebauer, and D. J. Perreault, "A fabrication method for integrated filter elements with inductance cancellation," *IEEE Trans. Power Electron.*, vol. 24, no. 3, pp. 838–848, Mar. 2009.

[10] H. Huang and T. Lu, "A cancelation method of mutual inductance between capacitors in EMI filter," *IEEE Trans. Power Electron.*, vol. 37, no. 10, pp. 11974–11984, Oct. 2022.

[11] P. González-Vizuete, J. Bernal-Méndez, M. J. Freire, and M. A. Martín-Prats, "Improving performance of compact EMI filters by using metallic and ferrite sheets," *IEEE Trans. Power Electron.*, vol. 36, no. 8, pp. 9057–9068, Aug. 2021.

[12] A. Kobayashi, S. Yuichi, and Y. Naofumi, "A new inductance cancelation scheme for surface mount shunt capacitor filters," *IEEE Trans. Electromagn. Compat.*, vol. 64, no. 3, pp. 732–740, Jun. 2022.

[13] R. Ludwig and P. Bretchko, *RF Circuit Design: Theory and Application*, 2nd ed. Englewood Cliffs, NJ, USA: Prentice-Hall, 2009.